Protoplasma (2006) 229: 53–62
DOI 10.1007/s00709-006-0183-1

PROTOPLASMA
Printed in Austria

Molecular cloning and gene expression of a fibrillarin homolog of tobacco BY-2 cells

Y. Makimoto, H. Yano, T. Kaneta, Y. Sato, and **S. Sato***

Department of Biology, Faculty of Science, Ehime University, Matsuyama

Received August 4, 2005; accepted November 2, 2005; published online October 6, 2006

Summary. Fibrillarin is known to play an important role in precursor ribosomal RNA processing and ribosome assembly. The present study describes a fibrillarin homolog gene isolated from tobacco BY-2 cells and its expression during the cell cycle. The cDNA for a fibrillarin homolog, named *NtFib1*, was first cloned in *Nicotiana tabacum* with degenerate primers. It encodes 314 amino acids and the deduced amino acid sequence has some highly conserved functional domains, such as the glycine and arginine-rich (GAR) domain for nucleolar localization and the RNA-binding motif. The C-terminal region is highly conserved and has 7 β-sheets and 7 α-helices which are peculiar to fibrillarin. Thus, it is suggested that the fibrillarin homolog of this plant species functions in the same way as the fibrillarin already known from human and yeast cells. Northern blot analysis of BY-2 cells synchronized with aphidicolin or a combination of aphidicolin and propyzamide showed that the histone H4 gene was specifically expressed in the S phase but *NtFib1* mRNA remained at high levels during the cell cycle. Examination of the localization of NtFib1 protein tagged with green-fluorescent protein (GFP) suggested that some persisting in the mitotic apparatus was eventually incorporated into reconstructed nucleoli in late telophase. Newly synthesized GFP-tagged NtFib1 protein in the cytoplasm was added to the recycled protein in early mitosis. Highly concentrated actinomycin D completely inhibited the transcription of genes coding for rRNA (rDNA) but did not significantly suppress the amount of either *NtFib1* mRNA or protein, although the NtFib1 protein was reversibly dislocated from nucleoli. Although hypoxic shock completely prohibited rDNA transcription, *NtFib1* mRNA remained at the same level as in the control experiment, even after the 4 h treatment. These results indicate that the transcription of *NtFib1* mRNA is not related to rDNA transcription and *NtFib1* mRNA is resistant to disrupting factors during the cell cycle.

Keywords: Actinomycin D; Cloning; Fibrillarin; Hypoxia; Nucleolus; *Nicotiana tabacum*.

Introduction

Fibrillarin is one of major components constituting the nucleolus. This acidic protein has a molecular weight of 34,000–38,000 and was first identified as B-36 in *Physarum polycephalum* (Christensen et al. 1977). Since then it has been detected in various types of cells (Lischwe et al. 1985, Ochs et al. 1985b, Guiltinan et al. 1988). Fibrillarin is specifically localized in the dense fibrillar component (DFC) of the nucleolus and associated with U3, U8, and U13 small nucleolar RNA (snoRNA) in human cells (Tyc and Steitz 1989). These snoRNA commonly have C(UGAUGA/U) and D(CUGA) boxes (Smith and Steitz 1997), which function as guide RNA for site-specific methylation by fibrillarin (Bousquet-Antonelli et al. 1997). The methylation of rRNA precursors has been suggested to play an important role in ribosome maturation in vertebrates (Maden and Hughes 1997). Tollervey et al. (1993) generated temperature-sensitive lethal point mutations in yeast fibrillarin and found that some alleles prevented synthesis of both 18S and 25S rRNA. Thus, it is believed that fibrillarin is involved in pre-rRNA processing and ribosome assembly. This suggests that there is a positive relation between transcription of genes coding for rRNA (rDNA) and the *NtFib1* gene.

Fibrillarin has been cloned from *Saccharomyces cerevisiae* and some animals, such as *Xenopus laevis*, humans, *Drosophila melanogaster*, and *Tetrahymena thermophila* (Schimmang et al. 1989, Lapeyre et al. 1990, Aris and Blobel 1991, David et al. 1997). The deduced amino acid sequences from these cDNAs exhibit some highly conserved domains and motifs, such as the glycine-arginine-rich (GAR) domain for nucleolar localization and the RNA recognition motif. Antibodies against human fibrillarin recognize 37 kDa proteins in onion cells (Cerdido and Medina 1995). Plant fibrillarin homolog genes were first cloned from *Arabidopsis thaliana* (Barneche et al. 2000, Pih et al. 2000). The deduced amino acid sequence of this fibrillarin homolog is very similar to fibrillarin and functional domains or motifs are also

* Correspondence and reprints: Department of Biology, Faculty of Science, Ehime University, Bunkyo-cho 2-5, Matsuyama 790-8577, Japan.
E-mail: ssato@sci.ehime-u.ac.jp

preserved. This suggests that fibrillarin homologs are present in a great variety of plant cells.

Fibrillarin has been suggested to be one of the argyrophilic proteins included in the nucleolus (Roussel and Hernandez-Verdun 1994). Argyrophilic proteins have been found to accumulate on the chromosome surface in anaphase and eventually be incorporated into the daughter nuclei (Sato 1985, 1988). Dundr et al. (2000) used fibrillarin tagged with green-fluorescent protein (GFP) to directly follow fibrillarin in living monkey CMT3 cells. Their results showed that fibrillarin was localized in perichromosomal regions in early anaphase and incorporated into tiny dots, putative nucleolar organizing regions, in late anaphase. In HeLa cells, GFP-tagged fibrillarin was found to be associated with the chromosome periphery and to travel in association with chromosomes during anaphase migration (Savino et al. 2001). Thus, fibrillarin is probably synthesized in mitosis and accumulates on the chromosomes. However, as fibrillarin mRNA is not transcribed in mitosis, its synthesis does not seem to be controlled at the transcriptional level.

The purpose of this study was to identify fibrillarin homolog genes in tobacco BY-2 cells and then to determine whether there is a relationship between rDNA transcription and gene expression of a fibrillarin homolog. The results show that inhibition of rDNA transcription did not reduce the amount of fibrillarin homolog mRNA and protein but that the mRNA is stable during mitosis.

Material and methods

Plant cell culture and synchronization

Tobacco BY-2 cells (*Nicotiana tabacum* L. cv. Bright Yellow 2) were grown in a modified Linsmaier and Skoog medium supplemented with 3% sucrose, 370 mg of KH_2PO_4, 1.0 mg of thiamine hydrochloride, and 0.2 mg of 2,4-dichlorophenoxyacetic acid per liter in an Erlenmeyer flask on a reciprocating shaker at 110 strokes per min at 25 °C, as described elsewhere (Nagata et al. 1981). For synchronization of the cell cycle at S phase, 20 ml of 7-day-old culture was added to 100 ml of medium containing 5 mg of aphidicolin (Wako, Osaka, Japan). The cells were cultured for 24 h and then washed with aqueous 3% sucrose solution. They were resuspended in fresh medium without aphidicolin and further cultured for 18 h. Synchronization of the cell cycle by the sequential aphidicolin-propyzamide treatment was basically the same as described by Kakimoto and Shibaoka (1988). Briefly, cells were first cultured for 24 h in medium containing 5 mg of aphidicolin per ml and washed with aqueous 3% sucrose solution. After 3.5 h in fresh medium without aphidicolin, propyzamide was added to a final concentration of 5 mM and the cells were cultured for further 6 h. They were then washed, resuspended in fresh medium, and further cultured for 18 h.

Measurement of mitotic index

Cells collected at given times from the synchronized suspension culture were fixed overnight at 4 °C in 3.7% formaldehyde in 0.067 M phosphate buffer (47 mM Na_2HPO_4 and 20 mM KH_2PO_4, pH 7.17). They were washed in 0.067 M phosphate buffer, stained for DNA with 1 μg of 4′,6-diamidino-2-phenylindole (DAPI) (Sigma, Steinheim, Federal Republic of Germany) per ml. More than 1000 cells were counted for measurement of the mitotic index using a fluorescence microscope equipped with a Nikon epi-illuminator (Tokyo, Japan).

Cloning and sequencing of fibrillarin cDNA

Total RNA was extracted from BY-2 cells using the Extract-A-Plant RNA isolation kit (Clontech, Palo Alto, Calif., U.S.A.). RT-PCR was performed using the total RNA, degenerate primers (5′-GAY GTI GCI CAR GC-3′ and 5′-GC RTG RTC ICK YTC RWA IGG YTC IAR IGT-3′) and Ready To Go RT-PCR beads (Amersham Biosciences, Tokyo, Japan) according to the GeneAmp PCR System 2400 manufacturer's instructions (Perkin-Elmer, Boston, Mass., U.S.A.). The amplified PCR products were subcloned using the TOPO TA cloning kit (Invitrogen, Carlsbad, Calif., U.S.A.). The inserts were confirmed to be putative fibrillarin gene fragments by sequencing with the BigDye Terminator Cycle Sequencing FS Ready Reaction kit (Applied Biosystems, Tokyo, Japan) and an ABI 310 sequencer (Applied Biosystems). The plasmid DNA containing the fibrillarin fragment was linearized by *Bam*HI and used as template for the generation of a probe. A digoxigenin (dig)-labeled RNA probe was generated by in vitro transcription using linearized template, DIG RNA labeling mix (Roche Diagnostics, Tokyo, Japan), and T7 RNA polymerase (Toyobo, Osaka, Japan). To obtain a full-length cDNA clone of the tobacco fibrillarin homolog, plaque screening was carried out using the tobacco BY-2 λZAP cDNA library (kindly provided by K. Mizuno, Osaka University) and a dig-labeled RNA probe. Positive cDNA clones were amplified by PCR using M13 forward and M13 reverse primers, and then the amplified fragments were cloned into the pCR 2.1 vector using the TOPO TA cloning kit. Sequencing of cDNA cloned into the pCR 2.1 vector was performed with the BigDye Terminator Cycle Sequencing FS Ready Reaction kit and the ABI 310 sequencer. Alignment of the deduced amino acid sequence of the full-length cDNA (named *NtFib1*, accession number AB207972) was performed by CLUSTAL W.

Generation of antisense RNA probe specific to NtFib1

PCR was carried out with cloned pCR 2.1 as template, primers (5′-AGCG GATAACAATTTCACC-3′ and 5′-AATTAACCCTCAACTAAACCC-3′) and KOD-plus-DNA polymerase (Toyobo). In vitro transcription for the generation of a dig-labeled antisense RNA probe was carried out at 37 °C for 2 h using purified PCR products and DIG RNA labeling mix. The reaction was stopped by addition of EDTA and the transcripts were precipitated with ethanol and NaOAc. The RNA probes were vacuum dried and then dissolved in autoclaved distilled water.

Northern blot analysis

Total RNA (5 μg) was separated by electrophoresis on 1.2% agarose formaldehyde gels. The RNAs were stained in gels with ethidium bromide and their profiles were photographed with a Polaroid camera or captured by a LAS-1000 UVmini (Fujifilm, Kanagawa, Japan). The RNAs were transferred onto nylon membranes (Hybond N+; Amersham Biosciences) and the membranes were rinsed in 2× SSC (300 mM NaCl, 30 mM tri-sodium citrate). They were dried in air and then exposed to ultraviolet light for 4 min using a UV Transilluminator (Vilber Lourmat, Marne La Vallee, France).

Hybridization was carried out overnight at 68 °C with antisense RNA probes specific for *NtFib1* mRNA or histone H4 mRNA. The antisense RNA probe for histone H4 mRNA was prepared from *Hordeum vulgare* L. cv. Akashinriki. The membranes were washed twice in 2× SSC containing 0.1% sodium dodecyl sulfate (SDS) for 5 min at 68 °C and were then washed twice for 15 min in 0.1× SSC containing 0.1% SDS at 68 °C. Signals were detected with the chemiluminescence detection kit using CSPD (disodium 3-(4-methoxyspiro{1,2-dioxetane-3,2′-(5′-chloro)tricyclo[3.3.1.1^{3,7}]decan}-4-yl)phenyl phosphate) as substrate (Roche

Diagnostics) and were exposed to X-ray film (Fujifilm) or incorporated by a LAS-1000 UVmini.

Inhibition of RNA transcription

Actinomycin D (AMD) (Wako) was dissolved in 50% ethanol to make a 5 mg/ml stock solution. First, we examined the relationship between AMD dose and DNA transcription. Cell suspension culture was treated with 0.05, 5, 25 or 50 mg of AMD per ml for 1 or 4 h. Immediately, [5′-^{3}H]uridine ([^{3}H]uridine) (Perkin-Elmer) was added to each suspension culture to a final concentration of 185 kBq/ml and incubated for a further 30 min. Total RNA extraction and electrophoretic separation of RNAs followed by transfer onto nylon membranes were performed as described above. For detection of radioactivity, fluorography was employed. The membrane was placed between the plastic films of a hybridization bag and was moistened with a liquid scintillation cocktail (Beckman Instruments, Fullerton, Calif., U.S.A.). The bag was then sealed and chemiluminescence signal was exposed to an X-ray film (Fujifilm) for 3–4 weeks at 4 °C in a desiccated dark box.

Hypoxic conditions have been suggested to inhibit RNA transcription (Fernandez-Gomez et al. 1984, Gimenez-Abian et al. 1985). Such conditions were attained by boiling the medium for 5 min and immediately cooling down to 25 ± 1 °C with cold tap water. Measurement with a dissolved-oxygen meter (Toa Electronics, Tokyo, Japan) indicated that the dissolved oxygen (O_2) concentration was approximately 1.5 mg/l. The treated medium was immediately poured into a vial (volume, 22 ml) and 0.7 g of fresh weight of 4-day-cultured cells was suspended in it. The vial was sealed with Parafilm and cells were cultured for 0.5, 1, 2, or 4 h at 25 °C in the dark without shaking. [^{3}H]uridine was added to each culture at a final concentration of 92.5 kBq/ml and the cells were incubated for a further 30 min. Radioactive signals were detected by fluorography as described above.

GFP::Ntfib1 construction, transformation, and selection of transformants

We used a Gateway binary vector pGWB6 (T. Nakagawa, Shimane University, Japan, unpubl.) for expression of the GFP::NtFib1 fusion protein. This vector was derived from pABH-Hm1 (Mita et al. 1995) by replacing the β-AmyP-GUS region with a sequence consisting of the cauliflower mosaic virus 35S promoter, sGFP and the R-cassette. Full-length *NtFib1* cDNA was amplified using a forward primer with an additional CACC sequence (5′-CACCATGGTTTGCACCAACTAGAGGTGG-3′) and a re-

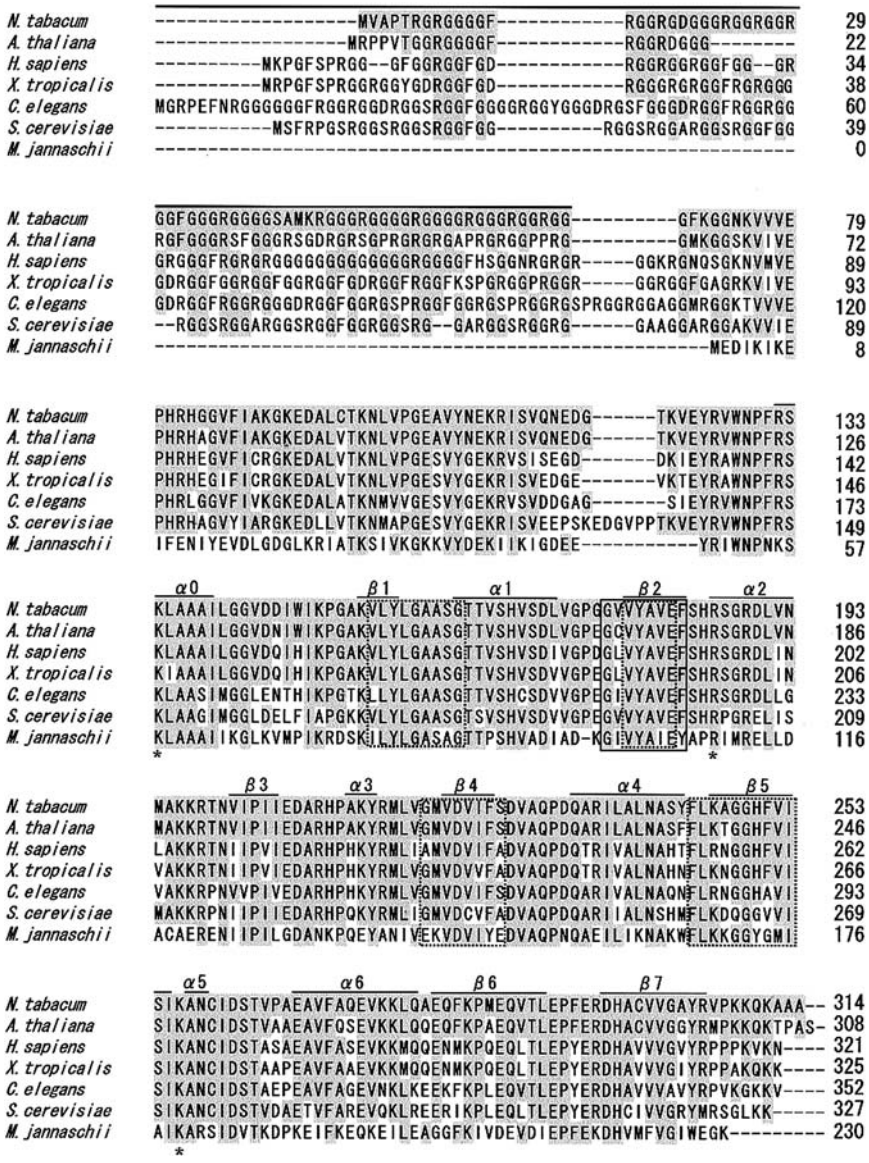

Fig. 1. Amino acid sequence alignment of fibrillarin homologs. The amino acids identical to residues in NtFib1 are shaded. The N-terminal glycine- and arginine-rich domain is overlined. The C-terminal region has 7 β-sheets and 7 α-helices. The RNA-binding motif is indicated by a solid-line box. Dotted-line boxes are conserved methyltransferase motifs (Niewmierzycka and Clarke 1999). Three positively charged residues (asterisks) are strictly conserved in the fibrillarin protein family. Sequence accession numbers are as follows: *Nicotiana tabacum*, AB207972; *Arabidopsis thaliana*, ATG5G52470; *Homo sapiens*, P22087; *Xenopus tropicalis*, NP_989101; *Caenorhabditis elegans*, Q22053; *Saccharomyces cerevisiae*, NP_010270; *Methanocaldococcus jannaschii*, NP_247681

verse primer with a stop codon (5′-CTAGGCAGCAGCCTTTTGCTT CTTT-3′), and pCR 2.1 containing *NtFib1* cDNA as a template. The resulting PCR product was cloned into the Gateway pENTR/D-TOPO cloning vector (Invitrogen) according to the manufacturer's instructions. The insertion of *NtFib1* cDNA was confirmed by sequencing. The pGWB6 vector and the entry vector containing *NtFib1* cDNA were used in an LR recombination reaction (Invitrogen) according to the manufacturer's instructions. The resultant expression vector was electroporated into *Agrobacterium tumefaciens*, which was used to transform tobacco BY-2 cells. Transgenic lines were obtained by selection with 100 μg of kanamycin per ml. The transformed BY-2 cells were maintained in modified LS liquid medium by subculturing every week, according to the standard BY-2 culture protocol (Nagata et al. 1992). The concentration of antibiotics was gradually decreased and transformed BY-2 cell lines, which grew at a speed similar to that of wild-type BY-2 cells, were established.

Fibrillarin-GFP localization was analyzed in cells fixed with 3.7% formaldehyde in 0.067 M phosphate buffer under a Nikon epifluorescence microscope. Images were captured by a cooled charge-coupled-device camera BS-41L (Britran, Saitama, Japan). Digital images were processed by deconvolution using Image-Pro Plus version 4.5 software (MediaCybernetics, Silver Spring, Md., U.S.A.).

Results

Characterization of the tobacco fibrillarin homolog

We first isolated a fibrillarin homolog cDNA from tobacco BY-2 cells and named it *Nicotiana tabacum* fibrillarin homolog (*NtFib1*). The cloned full-length *NtFib1* cDNA is about 1.2 kb and has an open reading frame for a protein of 314 amino acids. The deduced amino acid sequence of this protein was compared with fibrillarin-like proteins from various organisms (Fig. 1). NtFib1 shares 83% amino acid sequence identity with the *Arabidopsis thaliana* fibrillarin homolog, 73% with human fibrillarin, and 66% with yeast fibrillarin. It is 42% identical to *Methanocaldococcus jannaschii* fibrillarin. Although the amino acid sequences of fibrillarin homologs differ somewhat among organisms, NtFib1 retains all important functional domains and motifs peculiar to fibrillarin. Variations in the amino acids sequence are almost all restricted to the N-terminal region. However, this region contains the glycine- and arginine-rich domain (GAR domain), which is required for the nucleolar localization of this protein. The GAR domain is characterized by the typical consensus sequence GGR(G/D/S)(G/F). The C-terminal region of NtFib1 includes 7 β-sheets and 7 α-helices, like those from other organisms, and shows a higher degree of amino acid sequence homology with other fibrillarin homologs. This region has an important functional amino acid sequence forming the putative RNA-binding (GCVYAVEF) motif and several motifs from S-adenosyl-L-methionine (AdoMet)-dependent methyltransferase concerved in archaebacterial fibrillarin homologs (Deng et al. 2004). Three positively charged residues surrounding the AdoMet-binding site are strictly conserved in all of the fibrillarin protein family.

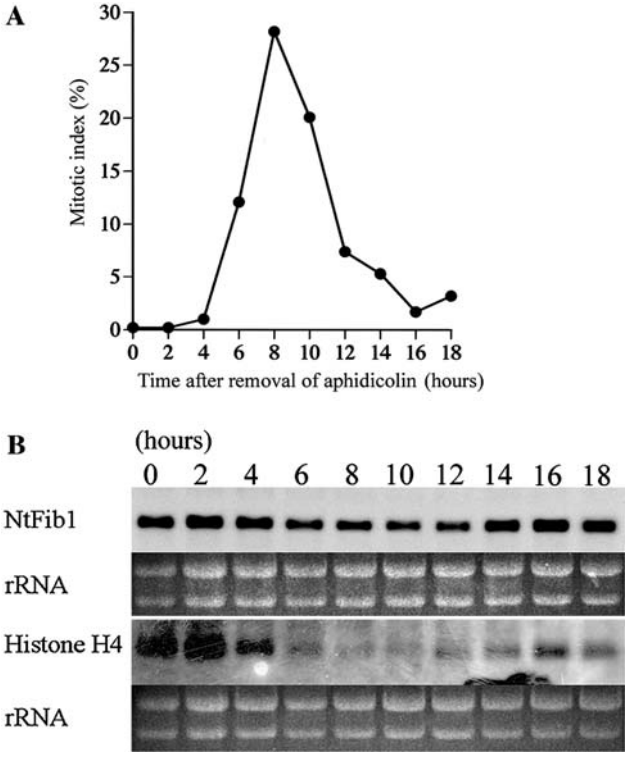

Fig. 2 A, B. Gene transcription of a tobacco fibrillarin homolog in cells synchronized by aphidicolin. **A** Mitotic index after release from the aphidicolin block. **B** Cells were collected for Northern blot analysis at time points corresponding to those indicated in panel A. Total RNAs (5 μg/lane) were electrophoretically separated on a 1.2% agarose gel, blotted, and hybridized with dig-labeled antisense RNA probes for the *NtFib1* and histone H4 genes. rRNA, stained with ethidium bromide, was used as a control and histone H4 expression was used as a marker for S phase. Signals for *NtFib1* mRNA are strong in S phase but are also present in mitosis

NtFib1 gene expression during the cell cycle

When the cell cycle of tobacco BY-2 cells was synchronized with aphidicolin, the mitotic index began to increase after 4 h and attained the highest value of about 30% at 8 h (Fig. 2). The histone H4 gene was expressed at high levels between 0 and 4 h and at low levels between 6 and 12 h after removal of aphidicolin. At 14 h, histone H4 mRNA transcription began to increase again. These results agree with the previous report that histone H4 mRNA transcription increases 3- to 10-fold above the basal level in G_1 phase (Heintz 1991). Thus, we roughly categorized the period from 0 to 4 h as the S–G_2 phase, 4 to 12 h as the mitotic phase, and 14 to 18 h as the G_1–S phase. *NtFib1* was strongly expressed in the S–G_2 and the G_1–S phases or interphase. In contrast to the histone H4 gene, however, *NtFib1* mRNA remained at high levels during the course of mitosis.

The high level of retention of *NtFib1* mRNA in mitosis may be due to incomplete synchronization of the cell cycle with aphidicolin. We, therefore, employed the double syn-

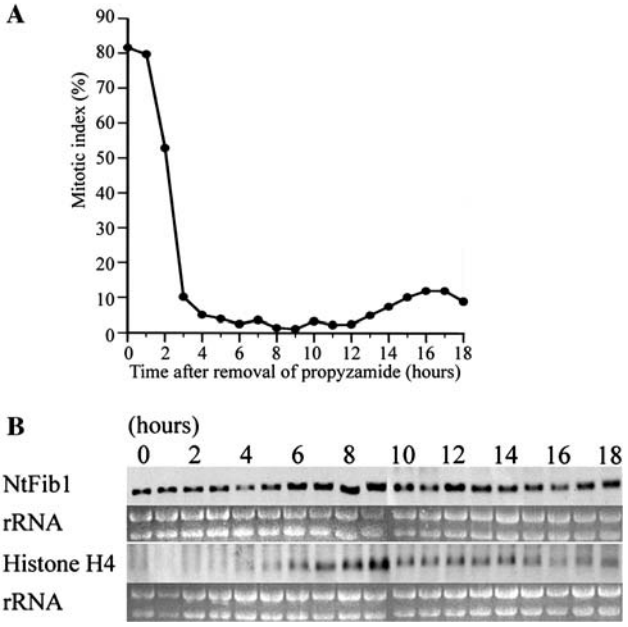

Fig. 3 A, B. Gene transcription of a tobacco fibrillarin homolog in cells synchronized by sequential aphidicolin-propyzamide treatment. **A** Mitotic index after release from the propyzamide block. **B** Cells were collected for Northern blot analysis at time points corresponding to those indicated in panel A. Total RNAs (5 μg/lane) were electrophoretically separated on a 1.2% agarose gel, blotted, and hybridized with dig-labeled antisense RNA probes for the *NtFib1* and histone H4 genes. rRNA, stained with ethidium bromide, was used as a control and histone H4 expression was used as a marker for S phase. Although no signal for histone H4 mRNA can be seen, *NtFib1* mRNA shows a strong signal in mitosis

chronization technique which first blocks cells at early S phase with aphidicolin and then at preprophase with propyzamide. This technique remarkably raised the mitotic index to about 80% at 0 and 1 h after release from propyzamide (Fig. 3). It then rapidly dropped to a low level at 3 h and increased again after 12 h. The histone H4 gene was scarcely expressed in the period from 0 to 3 h and specifically expressed between 4 and 12 h, with a notable peak at 9 h. Hence, we designated the period from 0 to 3 h as the mitotic phase and that from 3 to 12 h as the G_1–G_2 phase. Although signals for *NtFib1* mRNA were somewhat conspicuous in the middle of the G_1–G_2 phase or interphase, a large amount of the mRNA still persisted in the mitotic phase. Although the results suggest that *NtFib1* mRNA transcription takes place in the G_1–G_2 phase, it is not certain whether the high level of retention of *NtFib1* mRNA in mitosis reflects constitutive gene expression or *NtFib1* mRNA stability. This led us to examine the effects of inhibiting DNA transcription on the signals for *NtFib1* mRNA.

AMD is widely used to inhibit DNA transcription. This drug is dissolved in 0.5% aqueous ethanol solution; therefore, we first confirmed that the alcoholic solution did not perturb rDNA transcription (Fig. 4). AMD did not show any

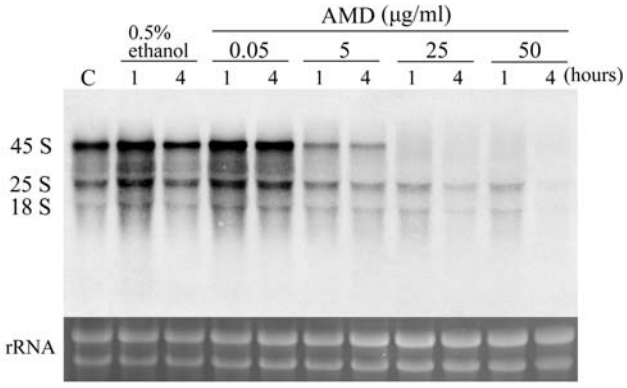

Fig. 4. Effects of AMD on rDNA transcription. AMD was added to the cell suspension at doses of 0.05, 5, 25, or 50 μg/ml and incubated for 1 or 4 h. Cells were immediately incubated for further 30 min in medium containing 185 kBq of [^{3}H]uridine per ml. Total RNA was extracted and electrophoretically separated on an agarose gel. Each lane was loaded with 20 μg of RNA. Separated RNAs were transferred onto a nylon membrane and radioactivity was detected by fluorography. rRNA, stained with ethidium bromide, was used as a control. The 0.5% ethanol that was used to dissolve AMD does not affect rDNA transcription. rDNA transcription is partially inhibited by 5 μg of AMD per ml and completely inhibited by 25 and 50 μg of AMD per ml. 45S, newly synthesized precursor rRNA; 25S and 18S, matured rRNAs

inhibitory effects on rDNA transcription at a concentration of 0.05 μg/ml. rDNA transcription was markedly suppressed by 5 μg of AMD per ml and it was completely inhibited by treatment with 25 and 50 μg of AMD per ml for 1 and 4 h. We examined *NtFib1* mRNA transcription in the presence of AMD at concentrations of 0.05, 5, 25, and 50 μg/ml for 10 h (Fig. 5). No significant change in the intensity of the *NtFib1* mRNA signals was seen at 0.05 μg/ml. Interestingly, the signals gradually increased at a dose of 5 μg/ml as the treat-

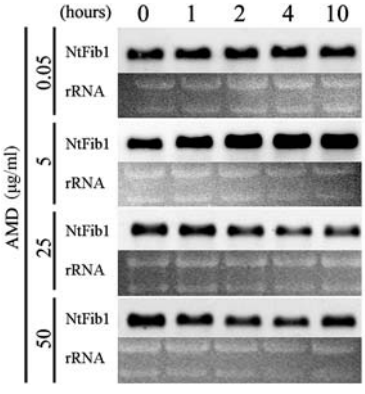

Fig. 5. Effects of AMD on *NtFib1* mRNA transcription. Cells were treated with 0.05, 5, 25, or 50 μg of AMD per ml for the indicated times and total RNA was immediately extracted. Total RNAs were electrophoretically separated on a 1.2% agarose gel. Each lane was loaded with 5 μg of RNA. *NtFib1* mRNA was then analyzed by Northern blot. rRNA, stained with ethidium bromide, was used as a control. No significant difference was seen in the signal at a dose of 0.05 μg/ml over 10 h. The *NtFib1* mRNA signal intensity gradually increased at a dose of 5 μg/ml but gradually decreased at doses of 25 and 50 μg/ml with increasing treatment time

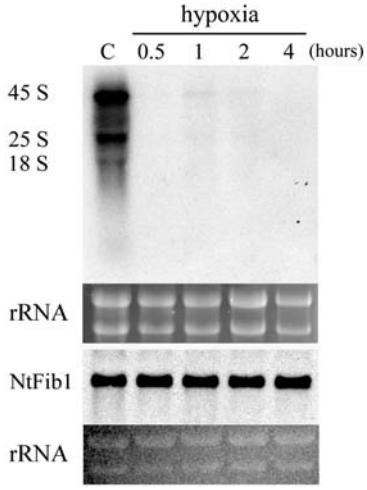

Fig. 6. Effects of hypoxia on *NtFib1* gene transcription. Cells were suspended in hypoxic medium and cultured for the indicated times without shaking. A final concentration of 92.5 kBq of [^{3}H]uridine per ml was added to the medium and culture was continued for an additional 30 min. Radioactive signals were detected by fluorography. rRNA, stained with ethidium bromide, was used as a control. DNA transcription was almost completely inhibited. *NtFib1* mRNA was detected by Northern blot analysis. The signal remained stable during the 4 h hypoxic treatment

ment time was prolonged. In contrast, *NtFib1* mRNA gradually decreased at concentrations of 25 and 50 μg/ml as the exposure time increased but persisted at least for 10 h at high levels (Fig. 5), although rDNA transcription was completely inhibited (Fig. 4).

The amount of *NtFib1* mRNA remained at the same level under hypoxic conditions for at least for 4 h, although rDNA transcription was completely blocked at 0.5 h and thereafter (Fig. 6).

Localization of the NtFib1 protein during the cell cycle

We examined how NtFib1 protein modifies its localization during mitosis (Fig. 7). The GFP-tagged NtFib1 protein began to diffuse as many spots from the nucleolus into the nucleoplasm in prophase. At metaphase, there was a strong GFP signal in the mitotic apparatus and a moderate one in the cytoplasm. The GFP signal became conspicuous around chromosomes in early anaphase and many bright spots began to appear here in late anaphase. These bright spots are apparently the structures previously called prenucleolar bodies (PNB) (Ochs et al. 1985a, Jimenez-Garcia et al. 1994). The small PNBs fused with each other to form large PNBs or the nucleolus during the course of telophase. They were eventually reconstructed into a single large nucleolus in interphase. Notably, the cytoplasm fluoresced moderately after metaphase until early anaphase but became dark in late anaphase. The cells transformed with the construct encoding

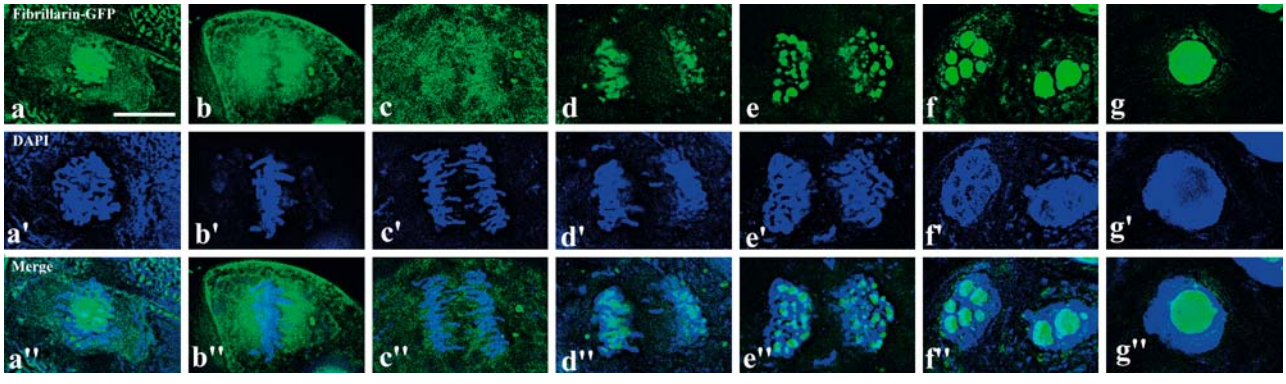

Fig. 7 a–g. Behavior of GFP-tagged NtFib1 proteins during the cell cycle. **a**, **a′**, and **a″** Prophase. **b**, **b′**, and **b″** Metaphase. **c**, **c′**, and **c″** Anaphase. **d**, **d′**, and **d″** Early telophase. **e**, **e′**, and **e″** Mid telophase. **f**, **f′**, and **f″** Late telophase. **g**, **g′**, and **g″** Interphase. GFP-tagged NtFib1 protein appears to disperse into the mitotic apparatus during the period from prophase to metaphase. The cytoplasm shows a moderate signal for NtFib1 protein. This disappears in anaphase with the concomitant appearance of an intense signal around chromosomes. The GFP-tagged NtFib1 protein forms spots similar to PNBs in telophase and these are eventually incorporated into the nucleolus in interphase. Bar: 10 μm

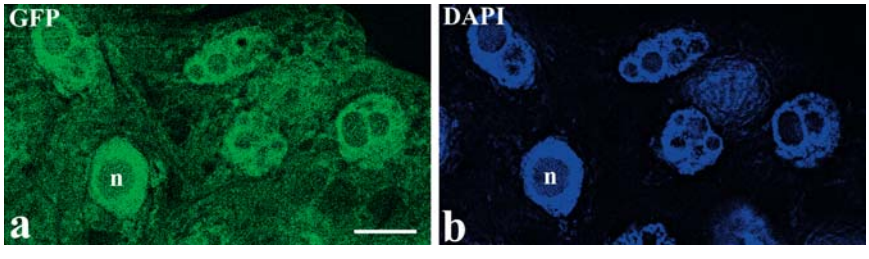

Fig. 8 a, b. Cells transformed with the GFP construct. The nucleoli (*n*) do not show bright fluorescence but the nucleoplasm is brightly stained. Bar: 10 μm

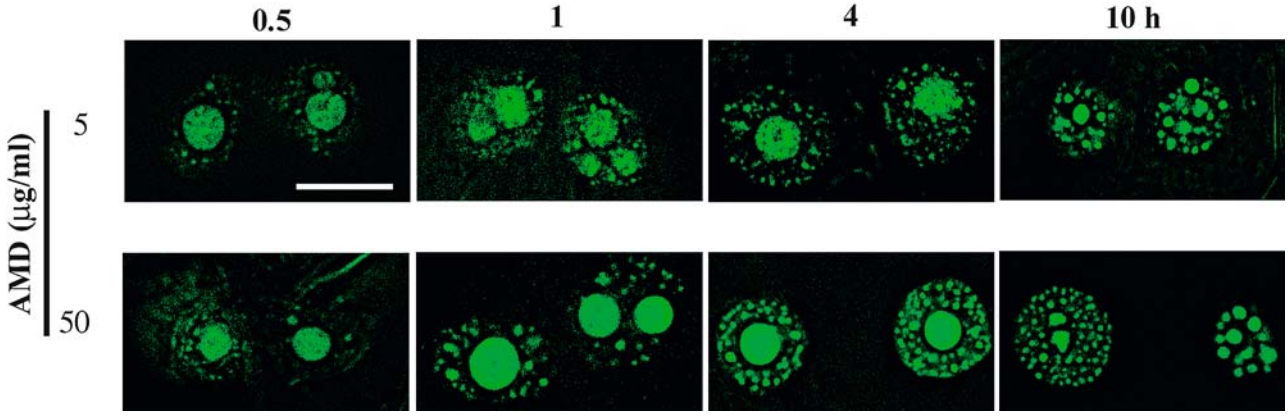

Fig. 9. Dislocation of GFP-tagged NtFib1 proteins from nucleoli into the nucleoplasm by treatment with AMD. Administration of AMD at concentrations of 5 and 50 μg/ml dislocates GFP-tagged NtFib1 protein from the nucleoli into the nucleoplasm, where it appears as many bright spots in a time-dependent manner. Bar: 10 μm

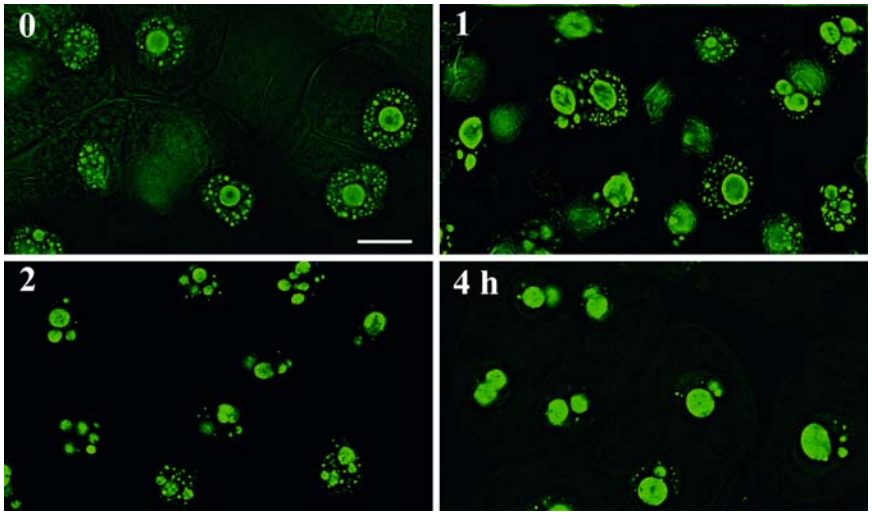

Fig. 10. Restoration of nucleoli after removal of AMD. Cells were first treated with 5 μg of AMD per ml for 6 h and then transferred to new medium without AMD. Many bright spots in the nucleoplasm were gradually incorporated into nucleoli. Bar: 10 μm

GFP alone showed strong fluorescence in the cytoplasm but not in the nucleoli (Fig. 8).

AMD reversibly changes the localization of NtFib1 protein

Tobacco BY-2 cells were continuously treated with 5 or 50 μg of AMD per ml and monitored at 0.5, 1, 4, and 10 h (Fig. 9). An abnormal appearance of the nucleolus was first distinguished at 0.5 h. Many green-fluorescent spots similar to the PNBs were seen around the nucleolus and they increased in number with the treatment time. The nucleolus sometimes broke into two or three nucleolar entities. After treatment for 10 h, the nucleolus completely disappeared and the nucleoplasm was filled with many bright spots. No difference in the timing of the appearance of bright spots was seen between treatment with 5 and 50 μg of AMD per ml.

When cells treated with 5 μg of AMD per ml for 6 h were transferred into new medium without AMD after washing in 3% sucrose solution, the bright spots gradually decreased in number and large spots appeared concomitantly (Fig. 10). After growth in AMD-free medium for 4 h, each cell contained one or two nucleoli but no bright spots. Thus, AMD reversibly dislocates NtFib1 proteins from the nucleolus into the nucleoplasm.

Discussion

Fibrillarin or its homologs have been recorded in only a few plant species. The present study is the first to describe a fibrillarin homolog in *N. tabacum*. The homology of the amino acid sequence of these proteins reflects the phylogeny of organisms. NtFib1 shows higher homology with the *Arabidopsis thaliana* fibrillarin homolog than with those of ver-

tebrates and the lowest homology with archaebacteria fibrillarin. Variability in the amino acid sequence is mostly restricted to the N-terminal region. However, NtFib1 retains all the domains and functional motifs common to human fibrillarin and yeast Nop1p. These include the N-terminal glycine- and arginine-rich domains required for nucleolar localization of nucleolus-targeted proteins. The C-terminal domain of NtFib1 is also very conserved and contains 7 β-sheets and 7 α-helices. *Saccharomyces cerevisiae* fibrillarin contains several motifs that are conserved in AdoMet-dependent methyltransferases (Niewmierzycka and Clarke 1999). The AdoMet-binding site is associated with three positively charged amino acid residues which are believed to interact with the negatively charged phosphate backbones of the snoRNAs (Deng et al. 2004). Amino acid sequences showing high homology with these motifs are also present in NtFib1. Wang et al. (2000) mapped temperature-sensitive mutations found in yeast fibrillarin to the *Methanococcus jannaschii* homolog and found that many of them are clustered in the core of the methyltransferase-like domain. Thus, it is believed that fibrillarin and fibrillarin homologs function as methyltransferases in pre-rRNA processing and ribosome assembly.

It has been reported that the histone H4 gene is specifically expressed in the S phase and its mRNA is unstable (Yang et al. 1994, Reichheld et al. 1998). This is largely in agreement with the present results, which show that histone H4 mRNA attained the culmination of its accumulation in the middle of the S phase but completely disappeared in mitosis. Northern blot analysis indicated that *NtFib1* mRNA remained at high levels throughout the cell cycle with a somewhat increased level in interphase. This high level of retention of *NtFib1* mRNA is expected to reflect *NtFib1* gene expression throughout the cell cycle and *NtFib1* mRNA stability.

AMD increased *NtFib1* mRNA signal intensity at a dose of 5 μg/ml for 10 h, while the signal decreased at doses of 25 and 50 μg/ml with increasing treatment time. AMD is known to exert different effects on DNA transcription depending on its concentration: it specifically inhibits rDNA transcription at lower concentrations, while the transcription of all types of RNA is disrupted at higher concentrations. The effective inhibition at lower concentrations is due to the high GC content of rDNA because AMD specifically binds to GC-rich double-stranded DNA, interfering with the action of RNA polymerase I (Ochs et al. 1985a, Dousset et al. 2000). Thus, 5 μg of AMD per ml effectively inhibits rDNA transcription but not DNA transcription into mRNA. The proportion of *NtFib1* mRNA to total RNA is, therefore, expected to increase at a dose of 5 μg of AMD per ml. On the other hand, 25 and 50 μg of AMD per ml slightly decreased *NtFib1* mRNA signal intensity during 10 h of treatment. Highly concentrated AMD may completely inhibit DNA transcription into mRNA (Nakagawa and Sakurai 2001, Masuda et al. 2003). In the present study, rDNA transcription was completely suppressed at doses of 25 and 50 μg/ml. Hence, the high level of retention of *NtFib1* mRNA throughout the cell cycle is probably not due to continuous transcription of the *NtFib1* gene but to the stability of *NtFib1* mRNA. *NtFib1* mRNA stability was also indicated by the effects of hypoxic treatment of the cells. When plants are submerged in preboiled water that has less than half the oxygen concentration of nonboiled water (Sato and Yamada 1996a), the nucleolus becomes clearly segregated into two regions, the dense fibrillar component and the granular component, in a short time and finally degrades after several hours (Sato and Yamada 1996b). It has been reported that hypoxic shock with preboiled water drastically reduces the ATP level in plant cells, prohibiting rDNA transcription (Fernandez-Gomez et al. 1984). This is supported by the present work: just 30 min exposure to hypoxia was enough to completely suppress rDNA transcription. In contrast, *NtFib1* mRNA remained at the same level during hypoxic treatment for at least 4 h. The Northern blot analysis using cells treated with AMD or hypoxia also indicated that inhibition of rDNA transcription does not cause a decrease in *NtFib1* mRNA transcription. This does not seem to be compatible with the idea that NtFib1 is required for pre-rRNA processing. However, plant fibrillarin has been suggested to be part of a complex that is able to process pre-rRNA (Saez-Vasquez et al. 2004).

The degradation of mRNA is an important determinant in the regulation of gene expression, especially for proteins that should be active for a short period, such as factors that control the cell cycle. A mechanism for transcript stability has been reviewed by Tourriere et al. (2002). They mention that the 5′ cap structure consisting of 7-methylguanosine bound at the 5′ end of the mRNA molecule by the 5′-5′-triphosphate linkage makes mRNA resistant to degradation by 5′ to 3′ exonucleases. Loop formation of mRNA also contributes to its stability: specific proteins associated with the 3′ poly(A) tail bind to the 5′ cap structure to inhibit decapping (Caponigro and Parker 1995, Muhlrad et al. 1995). Other factors have also been suggested to be involved in mRNA stability (Binder et al. 1994, Xu et al. 1997, Evdokimova et al. 2001).

The unusual behavior of fibrillarin during the cell cycle may require the stability of *NtFib1* mRNA. GFP-tagged fibrillarin in human cells has been found to be present at the chromosome periphery during mitosis and eventually

incorporated into the daughter nuclei (Savino et al. 1999). In early telophase, fibrillarin is concentrated in PNBs, which first assemble at the chromosome surface and then flow into the nucleolus (Savino et al. 2001). Pre-ribosomal ribonucleoproteins synthesized in the previous cell cycle may contribute to postmitotic nucleologenesis (Dousset et al. 2000). The present study of the localization of fibrillarin during the cell cycle also suggests that some of the previously synthesized fibrillarin persists through mitosis and is recycled for the formation of new nucleoli in the next cell cycle.

$HgCl_2$ has been shown to dislocate fibrillarin from the nucleolus in human cells (Chen and Mikecz 2000). The authors of that study argue that mercuric ions bind to subunits of RNA polymerase and thereby inhibit rRNA synthesis. This agrees with the present observation that inhibition of DNA transcription with AMD dislocates fibrillarin from the nucleolus to the nucleoplasm with the PNB-like structures. Interestingly, the nucleolus recovers when AMD is removed from the medium. The same result has been reported for human cells by Chen and Jiang (2004), who also showed that AMD causes dislocation of fibrillarin from nucleoli with small nucleoplasmic spots, but in this case the dislocation was reversible after removal of the drug from the medium. Thus, AMD treatment does not remarkably reduce the total amount of fibrillarin per cell in interphase, although it does dislocate it from the nucleolus.

GFP signals for fibrillarin were barely visible in the cytoplasm during the period from late anaphase to interphase, but this region exhibited a relatively high signal intensity from prophase to early anaphase. This suggests that fibrillarin newly synthesized in early mitosis migrates into the spindle or that some trapped in the spindle leaks out into the cytoplasm. Although it is possible that some of this protein comes from the nucleolus in the previous cycle, a proportion may be synthesized in mitosis and accumulate on the chromosome surfaces in anaphase to be incorporated into the daughter nuclei. Since *NtFib1* mRNA slightly increased in interphase, *NtFib1* gene transcription probably takes place in this period. As no DNA transcription occurs in mitosis, *NtFib1* mRNA is required to persist through mitosis for its translation in mitosis. Thus, this may be the reason why *NtFib1* mRNA remains stable during mitosis. We need to determine that *NtFib1* mRNA is actually translated in mitosis to confirm this conclusion.

Acknowledgment

We express sincere thanks to T. Nakagawa, Shimane University, for kindly providing us with the Gateway binary vector pGWB6.

References

Aris JP, Blobel G (1991) cDNA cloning and sequencing of human fibrillarin, a conserved nucleolar protein recognized by autoimmune antisera. Proc Natl Acad Sci USA 88: 931–935

Barneche F, Steinmetz F, Echeverria M (2000) Fibrillarin genes encode both a conserved nucleolar protein and a novel small nucleolar RNA involved in ribosomal RNA methylation in *Arabidopsis thaliana*. J Biol Chem 275: 27212–27220

Binder R, Horowitz JA, Basilion JP, Koeller DM, Klausner RD, Harford JB (1994) Evidence that the pathway of transferrin receptor mRNA degradation involves an endonucleolytic cleavage within the 3′ UTR and does not involve poly(A) tail shortening. EMBO J 13: 1969–1980

Bousquet-Antonelli C, Henry R, Glunge J-P, Caizergues-Ferrer M, Kiss T (1997) A small nucleolar RNP protein is required for pseudouridylation of eukaryotic ribosomal RNAs. EMBO J 16: 4770–4776

Caponigro G, Parker R (1995) Multiple functions for the poly(A)-binding protein in mRNA decapping and deadenylation in yeast. Genes Dev 9: 2421–2432

Cerdido A, Medina FJ (1995) Subnucleolar location of fibrillarin and variation of its levels during the cell cycle and during differentiation of plant cells. Chromosoma 103: 625–634

Chen M, Jiang P (2004) Altered subcellular distribution of nucleolar protein fibrilarin by actionmycin D in Hep-2 cells. Acta Pharmacol Sin 25: 902–906

Chen M, Mikecz A (2000) Specific inhibition of rRNA transcription and dynamic relocation of fibrillarin induced by mercury. Exp Cell Res 259: 225–238

Christensen ME, Beyer AL, Walker B, LeStrourgeon WM (1977) Identification of NG, NG-dimethylarginine in a nuclear protein from the lower eukaryote *Physarum polycephalum* homologous to the major proteins of mammalian 40S ribonucleoprotein particles. Biochem Biophys Res Commun 74: 621–629

David E, McNeil JB, Basile V, Pearlman RE (1997) An unusual fibrillarin gene and protein: structure and functional implications. Mol Biol Cell 8: 1051–1061

Deng L, Starostina NG, Liu ZJ, Rose JP, Terns RM, Terns MP, Wang BC (2004) Structure determination of fibrillarin from the hyperthermophilic archaeon *Pyrococcus furiosus*. Biochem Biophys Res Commun 315: 726–732

Dousset T, Wang C, Verheggen C, Chen D, Hernandez-Verdun D, Huang S (2000) Initiation of nucleolar assembly is independent of RNA polymerase I transcription. Mol Biol Cell 11: 2705–2717

Dundr M, Misteli T, Olson MOJ (2000) The dynamics of postmitotic reassembly of the nucleolus. J Cell Biol 150: 433–446

Evdokimova V, Ruzanov P, Imataka H, Raught B, Svitkin Y, Ovchinnikov LP, Sonenberg N (2001) The major mRNA-associated protein YB-1 is a potent 5′ cap-dependent mRNA stabilizer. EMBO J 20: 5491–5502

Fernandez-Gomez ME, Moreno Diaz de la Espina S, Risueno MC (1984) Nucleolar activity in anoxic root meristem cells of *Allium cepa*. Environ Exp Bot 24: 219–228

Gimenez-Abian MI, Rufas JS, de la Torre C (1985) The plant nucleolar cycle under hypoxia. Protoplasma 126: 47–53

Guiltinan MJ, Schelling ME, Ehtesham NZ, Tomas JC, Christensen ME (1988) The nucleolar binding protein B-36 is highly conserved among plants. Eur J Cell Biol 46: 547–553

Heintz N (1991) The regulation of histone gene expression during the cell cycle. Biochim Biophys Acta 1088: 327–329

Jimenez-Garcia LF, Segura-Valdez ML, Ochs RL, Rothblum LL, Hannan R, Spector DL (1994) Nucleologenesis: U3 snRNA-containing prenucleolar bodies move to sites of active pre-rRNA transcription after mitosis. Mol Biol Cell 5: 955–966

Kakimoto T, Shibaoka H (1988) Cytoskeletal ultrastructure of phragmoplast-nuclei complexes isolated from cultured tobacco cells. Protoplasma Suppl 2: 95–103

Lapeyre B, Mariottini P, Mathieu C, Ferrer P, Amaldi F, Almaric F, Caizergues-Ferrer M (1990) Molecular cloning of *Xenopus* fibrillarin, a conserved U3 small nuclear ribonucleoprotein recognized by antisera from humans with autoimmune disease. Mol Cell Biol 10: 430–434

Lischwe MA, Ochs RL, Reddy R, Cook RG, Yeoman LC, Tan EM, Reichlin M, Busch H (1985) Purification and partial characterization of a nucleolar scleroderma antigen (M_r = 34,000; pI, 8.5) rich in NG, NG-dimethylarginine. J Biol Chem 260: 14304–14310

Maden BE, Hughes JM (1997) Eukaryotic ribosomal RNA: the recent excitement in the nucleotide modification problem. Chromosoma 105: 391–400

Masuda Y, Yamada T, Marubashi W (2003) Time course analysis of apoptotic cell death during expression of hybrid lethality in hybrid tobacco cells (*Nicotiana suaveolens* × *N. tabacum*). Plant Cell Physiol 44: 420–427

Mita S, Suzuki-Fujii K, Nakamura K (1995) Sugar-inducible expression of a gene for β-amylase in *Arabidopsis thaliana*. Plant Physiol 107: 895–904

Muhlrad D, Decker CJ, Parker R (1995) Turnover mechanisms of the stable yeast PGK1 mRNA. Mol Cell Biol 15: 2145–2156

Nagata T, Okada K, Takebe I, Matsui C (1981) Delivery of tobacco mosaic virus RNA into plant protoplasts mediated by reverse-phase evaporation vesicles (liposomes). Mol Gen Genet 184: 161–165

Nagata T, Nemoto Y, Hasezawa S (1992) Tobacco BY-2 cell line as the "HeLa" cell in the cell biology of higher plants. Int Rev Cytol 132: 1–30

Nakagawa N, Sakurai N (2001) Cell wall integrity controls expression of endoxyloglucan transferase in tobacco BY2 cells. Plant Cell Physiol 42: 240–244

Niewmierzycka A, Clarke S (1999) S-Adenosylmethionine-dependent methylation in *Saccharomyces cerevisiae*. J Biol Chem 274: 814–824

Ochs RL, Lischwe MA, Shen E, Carrol RE, Busch H (1985a) Nucleologenesis: composition and fate of prenucleolar bodies. Chromosoma 92: 330–336

Ochs RL, Lischwe MA, Spohn WH, Busch H (1985b) Fibrillarin: a new protein of the nucleolus identified by autoimmune sera. Biol Cell 54: 123–134

Pih KT, Yi MJ, Liang YS, Shin BJ, Cho MJ, Hwang I, Son D (2000) Molecular cloning and targeting of a fibrillarin homolog from *Arabidopsis*. Plant Physiol 123: 51–58

Reichheld JP, Gigot C, Chaubet-Gigot N (1998) Multilevel regulation of histone gene expression during the cell cycle in tobacco cells. Nucleic Acids Res 26: 3255–3262

Roussel P, Hernandez-Verdun D (1994) Identification of Ag-NOR proteins, markers of proliferation related to ribosomal gene activity. Exp Cell Res 214: 465–472

Saez-Vasquez J, Caparros-Ruiz D, Barneche F, Echeverria M (2004) A plant snoRNP complex containing snoRNAs, fibrillarin, and nucleolin-like proteins is competent for both rRNA gene binding and pre-rRNA processing in vitro. Mol Cell Biol 24: 7284–7297

Savino TM, Bastos R, Jansen E, Hernandez-Verdun D (1999) The nucleolar antigen Nop52, the human homologue of the yeast ribosomal RNA processing RRP1, is recruited at late stages of nucleologenesis. J Cell Sci 112: 1889–1900

Savino TM, Gebrane-Younes J, Mey JD, Sibarita J-B, Hernandez-Verdun D (2001) Nucleolar assembly of the rRNA processing machinery in living cells. J Cell Biol 153: 1097–1110

Sato S (1985) Ultrastructural localization of nucleolar material by a simple silver staining technique devised for plant cells. J Cell Sci 79: 259–269

Sato S (1988) Formation of cytoplasmic nucleolus-like bodies from pre-existing nucleolar material in the mitotic cells of *Vicia faba*. Cell Biol Int Rep 12: 573–547

Sato S, Yamada M (1996a) Effect of hypoxia on nuclei in excised root tips of *Vicia faba*. Cytologia 61: 209–214

Sato S, Yamada M (1996b) Effect of hypoxia on nuclei in excised root tips of *Vicia faba*: an electron microscopic study. Cytologia 61: 269–276

Schimmang T, Tollervey D, Kern H, Frank R, Hurt EC (1989) A yeast nucleolar protein related to mammalian fibrillarin is associated with small nucleolar RNA and is essential for viability. EMBO J 8: 4015–4024

Smith CM, Steitz JA (1997) Sno storm in the nucleolus: new role for myriad small RNPs. Cell 89: 669–672

Tollervey D, Lehtonen H, Jansen R, Kern H, Hurt EC (1993) Temperature-sensitive mutations demonstrate roles for yeast fibrillarin in pre-rRNA processing, pre-rRNA methylation, and ribosome assembly. Cell 12: 443–457

Tourriere H, Chebli K, Tazi J (2002) mRNA degradation machines in eukaryotic cells. Biochimie 84: 821–837

Tyc K, Steitz JA (1989) U3, U8 and U13 comprise a new class of mammalian snRNPs localized in the cell nucleolus. EMBO J 8: 3113–3119

Wang HD, Boisvert KK, Kim R, Kim S-H (2000) Crystal structure of a fibrillarin homologue from *Methanococcus jannaschii*, a hyperthermophile, at 1.6 Å resolution. EMBO J 19: 317–323

Xu N, Chen C-HA, Shyu A-B (1997) Modulation of the fate of cytoplasmic mRNA by AU-rich elements: key sequence features controlling mRNA deadenylation and decay. Mol Cell Biol 17: 4611–4621

Yang W-C, Blank C, Mesklene I, Hirt H, Bakker J, Van Kammen A, Franssen H, Bisseling T (1994) Rhizobium Nod factors reactivate the cell cycle during infection and nodule primordium formation, but the cycle is only completed in primordium formation. Plant Cell 6: 1415–1426